

This discussion paper is/has been under review for the journal Atmospheric Chemistry and Physics (ACP). Please refer to the corresponding final paper in ACP if available.

Observations of total peroxy nitrates and total alkyl nitrates during the OP3 campaign: isoprene nitrate chemistry above a south-east Asian tropical rain forest

E. Aruffo^{1,2}, P. Di Carlo^{1,2}, C. Dari-Salisburgo¹, F. Biancofiore^{1,3}, F. Giammaria², J. Lee^{4,5}, S. Moller⁴, M. J. Evans⁶, J. R. Hopkins^{4,5}, C. Jones⁴, A. R. MacKenzie⁷, and C. N. Hewitt⁷

¹Center of Excellence CETEMPS Università degli studi di L'Aquila, Via Vetoio, Coppito, L'Aquila, Italy

²Dipartimento di Fisica, Università degli studi di L'Aquila, Via Vetoio, Coppito, L'Aquila, Italy

³Dipartimento di Chimica, Ingegneria Chimica e Materiali, Università degli studi di L'Aquila, Via Vetoio, Coppito, L'Aquila, Italy

⁴Department of Chemistry, University of York, York, YO10 5DD, UK

⁵National Centre for Atmospheric Science, Department of Chemistry, University of York, York, YO10 5DD, UK

4797

⁶ Institute for Climate and Atmospheric Science, School of Earth and the Environment, University of Leeds, LS28WE, UK

⁷ Lancaster Environment Centre, Lancaster University, Lancaster LA1 4YQ, UK

Received: 29 December 2011 – Accepted: 31 January 2012 – Published: 10 February 2012

Correspondence to: P. Di Carlo (piero.dicarlo@aquila.infn.it)

Published by Copernicus Publications on behalf of the European Geosciences Union.

Abstract

Measurements of total peroxy nitrates ($\Sigma\text{RO}_2\text{NO}_2$, ΣPNs), total alkyl nitrates (ΣRONO_2 , ΣANs) and nitrogen dioxide (NO_2) were made above the surface of a Malaysian tropical rain forest in Borneo, using a laser-induced fluorescence instrument developed at the University of L'Aquila (Italy). This new instrument uses the direct excitation of NO_2 at 532 nm in order to measure its concentrations detecting by the NO_2 fluorescence at wavelengths longer than 610 nm. ΣPNs and ΣANs are indirectly measured after their thermal dissociation into NO_2 . Observations showed enhanced levels of NO_2 during nighttime, an increase of ΣPNs during the afternoon and almost no evident diurnal cycle of ΣANs . The diurnal maximums of 200 pptv for ΣPNs and ΣANs are well below the peaks reported in other forest sites. A box model constrained with measured species, reproduces well the observed ΣPNs , but overestimates ΣANs concentrations. The reason of this model-observation discrepancy could be a wrong parameterization in the isoprene nitrates (INs) chemistry mechanism. Sensitivity tests show that: (1) reducing the yield of INs from the reaction of peroxy nitrates with NO to almost the lowest values reported in literature (5%), (2) reducing the INs recycling to 70% and (3) keeping the INs dry deposition at 4 cm s^{-1} , improve the agreement between modelled and measured ΣANs of 20% on average. These results imply that in the tropical rain forest, even if ΣPNs and ΣANs concentrations are lower than those observed in other North American forests, the yield and dry deposition of INs are similar. Another comparable result is that in the INs oxidation its recycling dominates with only a 30% release of NO_2 , which has implications on tropospheric ozone production and aerosol budget.

1 Introduction

Nitrogen oxides ($\text{NO}_x = \text{NO} + \text{NO}_2$) and total reactive oxidized nitrogen species ($\text{NO}_y = \text{NO}_x + \Sigma\text{RO}_2\text{NO}_2 + \Sigma\text{RONO}_2 + \text{HONO} + \text{NO}_3 + \text{N}_2\text{O}_5 + \dots$) play important roles in the chemistry of the troposphere, controlling the rate of ozone (O_3) production (Jacob,

4799

1999) and are core components of the tropospheric photochemical system. NO_x and O_3 are air pollutants and can cause damage to vegetation, ecosystems and the human health (EEA, 2005). In the troposphere, nitrogen oxide reservoirs ($\text{NO}_z = \text{NO}_y - \text{NO}_x$) are temporary sources and sinks for NO_x and their concentrations can determine the spatial extent of the O_3 production resulting from emissions of NO_x . For example, the main sink for NO_x is the oxidation of NO_2 carried out by OH producing nitric acid (HNO_3), which is water soluble and rapidly lost by wet deposition. In contrast, the formation of peroxyacetyl nitrate (PAN), which has a relative long lifetime, can affect the abundance of NO_x on global scale since it can be transported over long distances before it thermally decomposes (Crutzen, 1979; Hudman et al., 2004).

Various techniques are available to quantify the concentrations of nitrogen oxide reservoirs, the most common method is Photo-Fragmentation Chemi-Luminescence (PF-CL) (Fehsenfeld et al., 1987; Fahey, 1991; Williams et al., 1998). PF-CL instruments do not detect each NO_z individually, because they provide a total concentration, however, the speciation of the various components of NO_z is very important to understand chemical processes in the atmosphere. The concentrations of distinct NO_z like PNs and ANs are generally measured using different techniques like: (1) gas chromatography followed by electron capture detection (GC-ECD) (e.g. Roberts et al., 1998a; Atlas et al., 1993; Bertman et al., 1995; Flocke et al., 2005; Mills et al., 2007); (2) chemical amplification gas chromatography (CA-GC), which converts PAN to NO_2 and then uses luminol-based chemiluminescence to detect the latter (Blanchard et al., 1993); (3) ANs is also measured with gas-chromatography/mass spectrometry technique (GC/MS) (Reeves et al., 2007).

In the last decade a thermal dissociation system, followed by a laser-induced fluorescence (TD-LIF), has been used in several field campaigns for the concentration measurements of some NO_y types and, due to the TD-LIF fast response, for the quantification their fluxes, by using the Eddy Covariance technique (Day et al., 2002; Farmer et al., 2006). The TD-LIF is based on the heating of the air sample at different temperatures, in order to thermally dissociate three distinct NO_y types (ΣPNs , ΣANs and

4800

HNO₃) in turn to form NO₂, which is then measured by the LIF. Each NO_y compound has a characteristic dissociation temperature, due to different strengths of the X-NO₂ bond. Therefore ΣPNs, ΣANs and HNO₃ thermally dissociate into NO₂ at about 200 °C, 400 °C and 650 °C, respectively (Day et al., 2002). Secondary chemistry may have an impact on the observed NO₂ concentrations through the following three classes of reactions: (1) oxidation of ambient NO into NO₂; (2) reduction of NO₂ to NO and (3) oxidation of NO₂ (Day et al., 2002). Day et al.'s observations demonstrated that these interference processes can cause, at most, an error of 5 % in the measurements of ΣPNs, ΣANs and HNO₃. TD-LIF has become a well characterised technique for the measurement of NO₂ (particularly at low mixing ratios), ΣPNs, and ΣANs, and it can yield information important for the interpretation of atmospheric photochemistry. Wooldridge et al. (2010) reported a summary of the comparisons between TD-LIF observations of ΣPNs and individual PANs observed during several campaigns with different techniques. ΣPNs observed with TD-LIF agree to within 10 % with the summed individual PANs species and suggest that unmeasured PAN-type compounds are not evident in the atmosphere, as suggested by some photochemical mechanisms (Wooldridge et al., 2010).

Many experiments have investigated the NO_y budget, often in an attempt to find the “missing NO_y” (an unbalance between direct measurements of NO_y and the sum of the measured components) (Fahey et al., 1986; Ridley et al., 1990; Buhr et al., 1990; Trainer et al., 1991; Parrish et al., 1993; Williams et al., 1997). Using TD-LIF observations, Cohen's group found that ΣANs represent a large fraction of NO_y and their concentrations are enough to close the NO_y budget, at least in some sites (Day et al., 2003). In details: (1) at the Blodgett Forest Research Station (UC-BFRS), California (rural environment), Cohen's group found that ΣANs are 10–50 % of the total NO_y and about the amount of the “missing NO_y”; (2) at Granite Bay, California (suburban) and (3) La Porte, Texas (urban), where ΣANs represent 10–20 % and 8–20 % of the total NO_y, respectively (Day et al., 2003).

4801

The pool of volatile organic compounds (VOCs) emitted by vegetation is globally dominated by isoprene with estimated emissions of 440–660 Tg yr⁻¹ (Guenther et al., 2006). The oxidation of isoprene is efficiently initiated by OH, NO₃ and O₃, and the products of its oxidation chains impact NO_y budget, tropospheric O₃ and secondary organic aerosol (SOA) (Atkinson et al., 1983; von Kuhlmann et al., 2004; Fiore et al., 2005; Horowitz et al., 2007; Ito et al., 2007). Even if most of the products of the isoprene oxidation chains are known, the formation rate and fate of isoprene nitrates (INs) are still uncertain (Barnes et al., 1990; Horowitz et al., 2007; Paulot et al., 2009; Perring et al., 2009a; Rollins et al., 2009). INs are some of the minor channels of the isoprene oxidation chains but play a significant role in the level of tropospheric O₃, because of the NO_x sequestration associated with the INs formation, and on the aerosol budget, due to alkyl and multifunctional nitrates observed in the aerosol phase (Kroll et al., 2006; Day et al., 2008; Rollins et al., 2009). The yield of INs originated from the reaction of isoprene hydroxyperoxy radicals (some of the isoprene oxidation products) with NO may range between 4.4 % and 12 % (Horowitz et al., 2007; Perring et al., 2009a; Paulot et al., 2009). Other uncertainties are related with INs wet and dry deposition that are permanent sinks for NO_x. INs dry deposition used in different models varies between 0.4 and 5 cm s⁻¹ (Giacopelli et al., 2005; Rosen et al., 2004). Another factor that influences the INs chemistry is the recycling of INs when INs react with OH or O₃. Recent field campaigns and model simulations have put some constraints on the yield, recycling and dry deposition of INs: (1) Horowitz et al. (2007), using aircraft observations during the ICARITT campaign (USA), found that the best agreement between observed and modelled ΣANs (that includes also INs) is achieved using the following parameters: INs yield of 4 %, 50 % of INs recycling and a dry deposition of INs close to that of HNO₃ (4–5 cm s⁻¹); (2) Perring et al. (2009a), analysing aircraft observations taken over the US during the INTEX-NA campaign, almost confirmed Horowitz et al. (2007) results, stating that a low INs yield (4.4 %), a fast dry deposition (4–5 cm s⁻¹) and a recycling efficiency of 67 % are the parameters by which the best agreement between observed and modelled ΣANs is obtained. Perring et al. (2009a)

4802

also pointed out that Σ ANs (that include also INs) have a longer lifetime than single IN, which suggests a possible second oxidation cycle of organic nitrates.

In this paper we describe the enhancement of an existing NO_2 -LIF instrument developed at University of L'Aquila (Italy). The TD-LIF is a system for continuous measurements of NO_2 , Σ PNs and Σ ANs with high frequency sampling (10 Hz) and a detection limit of 3.6 pptv, 11.2 pptv and 13.1 pptv for NO_2 , Σ PNs and Σ ANs, respectively. The TD-LIF instrument was deployed during the July 2008 OP3 (Oxidant and Particle Photochemical Processes above a South-East Asian tropical rain forest) campaign in the Borneo rainforest (Malaysia) with the aim of investigating the role of isoprene oxidation products in the Σ ANs budget. The Dynamically Simple Model of Atmospheric Chemical Complexity (DSMACC) (Emmerson et al., 2009), developed at the University of Leeds, is used to model Σ PNs and Σ ANs. Observed LIF data are compared with the model outputs to estimate the INs yield from isoprene hydroxyperoxy radicals reaction with NO, which in some aircraft campaigns seems to be close to 4.4 %, but in experiments that use a controlled reaction chamber, it is estimated to be up to 12 % (Paulot et al., 2009). Constraints on the dry deposition of INs and the INs recycling when INs react with OH and O_3 are discussed using results and sensitivity tests of the DSMACC model.

2 Site description and instrumentation

The measurements reported in this work were carried out in July 2008 during the third international OP3 campaign on the 100 m tall tower of the Bukit Atur World Meteorological Organisation/Global Atmospheric Watch station (4° 58'49.33" N, 117° 50'39.05" E, 426 m a.s.l.) (<http://gaw.empa.ch/gawsis/>) in south-east Sabah, Malaysia. The Bukit Atur Global Atmospheric Watch (GAW) site chosen for the OP3 sampling is situated at an altitude of 437 m above mean sea-level, on a small hill approximately 260 m above the surrounding valley floor. Bukit Atur is within the Permanent Forest Estate (PFE) Production Forest of the Ulu Segama – Malua Forest Reserve, but is less than

4803

5 km east of the 438 km² area of PFE Protection Forest, known as the Danum Valley Conservation Area (DVCA). It is approximately 70 km inland from the town of Lahad Datu on Sabah's east coast. The DVCA covers 43 800 hectares and comprises almost entirely lowland dipterocarp forest; it represents the largest expanse of pristine forest of this type remaining in Sabah. This region has an equatorial climate with a mean annual temperature of 26.8 °C (mean monthly temperatures range from 25.8 °C in January and 27.6 °C in April) and a mean relative humidity of 78 % (14:00 LT) and 95 % (08:00 LT). The mean annual rainfall (1985–2006) is 2825 mm. More details on the site and measurements made during OP3 can be found in Hewitt et al. (2010). The general purpose of the OP3 project was to understand the mechanisms of reactive gases emissions from a tropical rainforest and how they affect the production and the chemistry of oxidants and particles in the local and global troposphere. A full description of the project objectives and an overview of the main results are reported in Hewitt et al. (2010).

The TD-LIF instrument of the University of L'Aquila (Italy) was operated during the period 1–23 July 2008, to measure NO_2 , Σ PNs and Σ ANs at about 8 m above the ground level at a rate of 1 Hz. The NO_2 mixing ratio was also measured at 75 m with a detection rate of 10 Hz in order to calculate NO_2 fluxes (Fowler et al., 2011). The NO_2 measurements at 75 m were made by switching the Σ ANs detection cell to sample NO_2 at 75 m for 25 min and Σ ANs for 3 min. In the OP3 configuration, the relative detection limits of for NO_2 , Σ PNs and Σ ANs were 3.6 pptv, 11.2 pptv and 13.1 pptv (60-s time averaging), respectively.

The TD-LIF system is an evolution of the NO_2 -LIF instrument developed at the University of L'Aquila (Italy) and described in details elsewhere (Dari Salisburgo et al., 2008). Briefly, it consists of: (1) a light source (Q-switched Laser, NavigatorTM I Spectra-Physics, at 532 nm; 3.8 W of power, 15 kHz of repetition rate and 20 ns of pulse-width); (2) detection cells; (3) a vacuum system; (4) an inlet box that includes the dissociation system and (5) a control system. To operate in the tropics, the system was installed in an air conditioned laboratory. The laser beam is steered by two high

4804

reflectivity mirrors (99% at 532 nm and 45 degree) before entering the first detection cell through a 5 cm diameter window, and leaves the other side of the cell through another antireflection window. In this configuration the laser radiation is sent sequentially through three cells: after each cell the beam is steered into the subsequent cell using high reflectivity mirrors. The laser power is monitored before and after each cell by four photodiode detectors (UDT55) to compensate the fluorescence counts for the laser power changes. More information about the LIF system, its controller and the calibration system can be found in Dari Salisburgo et al. (2008). Here the new components (the inlet and the dissociation system) are discussed. The dissociation system is used to thermally convert the Σ PNs and the Σ ANs into NO_2 ; ambient air is sampled through an inlet (a PFA tube, 56 cm long, 6.4 mm OD and 3.8 mm ID) (Fig. 1) and, subsequently, it is split into 3 equal flows to pass through three quartz tubes (120 cm long, 6.0 mm OD and 3.8 mm ID). The first quartz tube is not heated; the second and third ones are heated for the first 15 cm with a coiled nichrome wire (28 AWG, 13 ohms m^{-1} , ~ 60 ohms) to which 220 V AC is applied through a power controller (STOM 1, United Automation) in order to heat the inflowing ambient air. The temperatures are measured by thermocouples and controlled using a proportional-integral-derivative technique that modulates the current of the STOM. The thermocouples are fixed on the external surface of the quartz tube and are used to provide the feedback to the heater controller. Since the measured temperature is always lower than the effective temperature of the flow, the temperature intervals for the complete thermal dissociation of Σ PNs and Σ ANs compounds (200 °C and 400 °C, respectively), are determined by injecting known amounts of these species into the system and looking at the relative temperature of dissociation. The unheated first tube is used to measure the ambient NO_2 concentration; the second and the third tubes are heated at about 200 °C and 400 °C, respectively in order to dissociate Σ PNs and Σ ANs compounds into NO_2 (Day et al., 2002). The heated gas sample is cooled along the remaining quartz tube until it reaches a PFA Swagelok connector that reduces the air pressure. The sample air reaches a stainless steel nozzle in the detection cell, after passing through 10 m of

4805

1/4" PFA tube. In order to test the dissociation temperatures, several qualitative and quantitative laboratory tests were carried out. For example, in one of the quantitative tests, known concentrations of n-propyl nitrate (one of the Σ ANs) diluted in ultrahigh purity zero air were sampled by the instrument inlet. Figure 2 shows the result of this laboratory experiment: the instrument cells were kept at ~ 7.5 Torr pressure with a sensitivity of 40.14 Counts/(s ppb) and a mean error of $\sim 23.3\%$. A standard cylinder of n-propyl nitrate (0.997 ppm ($\pm 5\%$)) was diluted in zero air to sample ~ 2.3 ppb of n-propyl nitrate. Figure 2 shows the concentrations of n-propyl nitrate sampled with relative errors (calculated by propagating the contribution of each error), and the detected NO_2 produced by the TD-LIF thermal dissociation system with relative errors versus the heater temperature. The agreement between the amount of n-propyl nitrate sampled and the NO_2 , detected after the thermal dissociation of the former, proves the conversion efficiency of the system for this AN. The small concentration of NO_2 measured below 250 °C is due to some residual NO_2 present in the cylinder of n-propyl nitrate. Several laboratory tests were made in order to verify that both the zero air signal and calibration constant values do not change when ambient air is heated; in this way it has been possible to demonstrate that thermal dissociation is a selective method for the exclusive dissociation of the compounds of interest (Σ PNs, Σ ANs and HNO_3). An intercomparison between the LIF and chemiluminescent analyzer for NO_2 has already been described in details (Dari-Salisburgo et al., 2008), here we focus on the intercomparison between TD-LIF and a chemiluminescent analyzer for NO_z (CHEM- NO_z) based on the measurements carried out in summer 2008 during the OP3 campaign. In the CHEM- NO_z all the NO_y species are converted into NO by catalytic reduction using a CON 765Y NO_y converter. The converter contains a solid gold tube which is heated at 300 °C and housed in a section of a glass tubing. A low concentration of CO gas is mixed with the sample gas which flows through the glass tubing and over the gold surface where the wanted reduction is achieved. The produced NO is then measured by an Ecophysics CLD 780 TR chemiluminescence detector. The NO_x is measured by a second Ecophysics CLD 780 TR connected to an Ecophysics PLC 762

4806

NO₂ photolytic converter. NO_z concentration is usually calculated from the difference between NO_y and NO_x concentrations, but it can also be calculated using the single species measured by the TD-LIF:

$$\text{NO}_z = \text{NO}_y - \text{NO}_x = \Sigma\text{PNs} + \Sigma\text{ANs} + \text{HNO}_3 \quad (1)$$

5 Figure 3 shows the scatter plot between the NO_z obtained using NO_y and NO_x concentrations, measured by the CHEM-NO_z, and the NO_z calculated as the sum of ΣPNs and ΣANs, measured by the TD-LIF. In order to compare the data measured by different instruments, the analysis procedures required some manipulations of the raw data: the
10 shown CHEM-NO_z data are the 10-min median of the measured raw data, which were therefore compared with 10-min median TD-LIF data. The measurements used for the intercomparison in Fig. 3 were observed during the period 19–23 July 2008. A linear regression analysis between the NO_z measured by CHEM-NO_z and TD-LIF shows that the two sets of measurements have a correlation (*R*) of ~0.64 and a slope of ~0.99. Unfortunately, during OP3, speciated PANs measurements to be compared with TD-
15 LIF ΣPNs were not available, and the NO_z observed by the TD-LIF missed HNO₃, NO₃ and HONO. Therefore the low correlation between CHEM-NO_z and TD-LIF is the combination of the low selectivity of the CHEM-NO_z system and the missing species observed by the TD-LIF, in the OP3 configuration. Even if the correlation and slope between the chemiluminescence system and the TD-LIF observations are somehow
20 encouraging, a more selective intercomparison has been planned, to test the reported good agreement (within 10%) of the Berkeley TD-LIF measurements of ΣPNs and total speciated PANs species (Wooldridge et al., 2010).

3 Results and discussion

25 Figure 4 shows the diurnal cycle of NO₂, ΣPNs, ΣANs, O₃ and isoprene measured at 8 m from the surface at the Bukit Atur tower. This altitude has been selected because previous observations suggested that the Bukit Atur measurements made at 5 m and

4807

above are representative of the daytime mixed layer, hypothesis confirmed by the observations during OP3 (Pugh et al., 2010; Hewitt et al., 2009). At night, the hilltop of Bukit Atur was typically situated in a stable atmospheric layer decoupled from a
lower fog-filled stable layer that filled the surrounding valleys (MacKenzie et al., 2011;
5 Pearson et al., 2010). NO₂ concentration decreases during the day, with minimum values at around 0.2 ppbv between 12:00 LT and 16:00 LT and starts to increase in the late afternoon until it reaches maximum values of ~0.58 ppbv at around 22:00 LT (Fig. 4). Nocturnal concentrations of NO_x and O₃ in this site are driven by a small (about
10 $2.8 \times 10^9 \text{ molecules cm}^{-2} \text{ s}^{-1}$) local NO_x source from soil, a modest (about 1 mm s^{-1}) deposition of O₃ on the forest leaf surfaces, and a strongly reduced vertical mixing in the stable nocturnal air on the surface (Pugh et al., 2011). During the day, the photo-oxidation of biogenic VOCs, in particular isoprene, in a well-mixed boundary layer about
15 800 m deep, is also important (Pugh et al., 2010). The absence of anthropogenic NO_x sources, suggests an almost constant daytime NO_x emission with a predominant loss during the day due to photochemistry, evident from the increase of O₃. The nighttime increase of NO₂ concentrations and the persistent relatively high concentrations of O₃ after dusk can be explained with ozone deposition and soil emission of NO into a nocturnal atmosphere that is strongly stable in the first 20 m or so (Pugh et al., 2011).
20 The isoprene flux is triggered by temperature and sunlight variation (Guenther et al., 2006), therefore isoprene concentration starts to increase after the sunrise and keeps rising up to more than 2 ppbv (after 15:00 LT), and then it declines when temperature and sunlight drop (Fig. 4). The diurnal evolution of ΣPNs is similar to the isoprene one with a small temporal shift but both species reach the highest concentrations at the same time (Fig. 4). The similarity between the diurnal cycles of ΣPNs and isoprene is a qualitative confirmation that most of the ΣPNs compounds are produced
25 from the oxidation of isoprene intermediates like methacrolein (MACR) and methylvinyl ketone (MVK) (LaFranchi et al., 2009). ΣANs diurnal cycle is less evident compared to those of ΣPNs and isoprene, and the nighttime ΣANs high concentrations can be explained through the high efficiency of isoprene nitrates production due to the reaction

of isoprene with NO_3 (yield of about 65 %) that is abundant during the night (Perring et al., 2009b).

Observed data are analysed using a tropospheric chemistry box model called DSMACC (Emmerson et al., 2009; Stone et al., 2010) designed to study the composition of the troposphere and it can be used to calculate the expected concentrations of atmospheric species. The model uses the Kinetic Pre-Processor (KPP) (Damian et al., 2002), which is a software tool that assists the computer simulation of chemical kinetic systems. The Tropospheric Ultraviolet and Visible radiation model (TUV) (Madronich, 1987) provides the calculations of the photolysis rate. The chemical scheme of the DSMACC can be easily changed, for this reason it is possible to use it to compare different chemistry schemes. The DSMACC can be used both for free running and for constrained simulations. In the first case the concentrations of the species can vary freely from their initial conditions; in the second case it is possible to choose the species to be constrained in the model. The chemistry scheme used in the simulations reported here is the Master Chemical Mechanism (MCM) v3.2 (Jenkin et al., 2003; Saunders et al., 2003; Archibald et al., 2010; <http://mcm.leeds.ac.uk>), which is a near-explicit chemical mechanism describing the degradation of isoprene and other biogenic VOCs in details. The MCM describes the degradation of 135 primary VOCs, including isoprene and other biogenic VOCs. Isoprene accounts for 80 % (as carbon) of the measured emissions of reactive carbon fluxes from the forest (Langford et al., 2010). This scheme contains approximately 5600 species and 13 500 reactions which are defined on the basis of predefined protocols.

The constrained version of the model was used to simulate the average daytime trends of ΣPNs and ΣANs . Simulating the nighttime chemistry is complicated by the boundary layer dynamics (Pugh et al., 2010). The simulated time period ranging from 08:00 to 18:00 was divided into 20 steps of 30 min each. Each point is characterized by several parameters which represent the initial conditions. The parameters used in the simulations are: temperature, latitude, longitude, day of the year, atmospheric pressure, photo-dissociation of ozone (J-values), JO^1D , and the concentrations of some

4809

species: CO , H_2O , O_3 and some VOCs (Hopkins et al., 2003; Jones et al., 2011). The values of the parameters above are mean data, calculated for every step using the values measured during the OP3 campaign. Table 1 summarizes the input data. The concentration of CH_4 was set to 1770 ppm and the concentration of H_2 was set to 550 ppm since they do not change during the simulation. As regard the concentration of NO_x , for every step the model corrects the total concentration to ensure that it remains constant, whereas the concentration of other species can vary. At the end of each day the calculated concentration of NO_2 is compared to the measured NO_2 concentration, and the concentrations of all NO_x species are fractionally increased or decreased so that the measured and the modelled concentrations match. Unmeasured species are initially set at zero. The J-values used are calculated by the TUV model, assuming a constant ozone column of 260 Dobson units and an albedo of 0.1, and scaled according to the measured JO^1D . The model is integrated forward in time until a diurnal steady state is reached, this occurs when the daily mean fractional difference of the concentration of each unconstrained species and the daily mean fractional difference of the sum of all the species concentrations between a day and the previous are less than 0.01. Full details can be found in Stone et al. (2011). All the species in the model include a loss which can be considered like a continuous deposition process, such as dry deposition or mixing at zero concentration background. The height of the boundary layer we consider is 800 m (Pugh et al., 2010). For ΣPNs we use a deposition velocity of 4 cm s^{-1} that equals a loss rate of $5 \times 10^{-5} \text{ s}^{-1}$. The ΣANs dry deposition is set as that of ΣPNs , which is consistent with the daytime values reported elsewhere (Munger et al., 1996; Farmer et al., 2008). The dry deposition velocity of the INs is as that of ΣANs (4 cm s^{-1}). The first-order loss rates of the other species are set at $1 \times 10^{-5} \text{ s}^{-1}$ (Stone et al., 2010).

The model simulations, carried out using the parameters above plus recycling of INs of 100 % (meaning negligible NO_2 production from INs reaction with OH, O_3 and NO_3) and 10 % of INs yield from the reaction of isoprene hydroxyperoxy radicals with NO, can be considered the “base” simulations because they use the default parameters of

4810

the MCM. The processes that control the production and loss of Σ PNs during daytime, using the “base” simulations, are reported in the upper panel of Fig. 5. The main sink of Σ PNs is their thermal decomposition, whereas the reaction of NO_2 with acyl peroxy radicals is the main Σ PNs source. The lower panel of Fig. 5 shows the processes controlling the production and loss of Σ ANs during daytime. The main Σ ANs loss is the dry deposition (labelled as “DUMMY” in Fig. 5, according to the KPP labels, Damian et al., 2002). The reactions between isoprene peroxy radicals (ISOPAO₂, ISOPBO₂, ISOPCO₂ and ISOPDO₂) and NO are the main sources of Σ ANs. Figure 6a shows the diurnal cycle of the Σ PNs, calculated by the model using default parameters (labelled as “base”) and measured by the TD-LIF. Daytime concentrations of Σ PNs calculated by the model are in good agreement with the measured values between 12:00 and 16:00, with overestimations before and after this period. Figure 6b shows the diurnal cycle of Σ ANs calculated by the model, using default parameters (as “base”) and measured by TD-LIF. The model underestimates the observed Σ ANs for the first two hours of the simulation, whereas systematically overestimates them after 10:00 LT. From the processes that control the production and loss of Σ ANs (Fig. 5) it is possible to suppose that the uncertainties in the dry deposition, the yield of INs from the reaction of peroxy radical with NO and INs recycling are the reasons for the modelled-observed Σ ANs disagreement. To find the parameters that have an impact on the INs chemistry, sensitivity tests were performed changing the dry deposition, recycling and yield of INs and comparing how the agreement between measured and modelled Σ ANs changed. The starting point was the model output using the default parameters of the MCM for INs (dry deposition: 4 cm s^{-1} , recycling: 100 %, and yield from peroxy nitrates reaction with NO: 10 %), which had a sum of the squared differences (SSD) between modelled and measured Σ ANs of 0.15. Reducing the recycling to 70 % the SSD did not change significantly dropping only to 0.14; halving the INs dry deposition the SSD became worse (0.22), whereas halving the INs yield to 5 % the SSD achieved the best value (0.12). These tests suggest that the INs yield of 5 %, its recycling of 70 % and its dry deposition of 4 cm s^{-1} is the set of parameters that gives the best agreement between

4811

measured and modelled Σ ANs, as shown in Fig. 6b (line labelled “yield 5 % and recycle 70 %”). Changes in the recycling and deposition of INs do not impact the modelled Σ PNs that for both give the same SSD as the “base” simulation (0.09), only halving the INs yield to 5 % impacts a bit the SSD of Σ PNs that rises to 0.10 as shown in Fig. 6a (line labelled “yield 5 % and recycle 70 %”). These results confirm the results reported by Perring et al. (2009a) where they find the best agreement between measured and modelled Σ ANs when recycling of INs is 67 %, its yield 4.4 % and its dry deposition between 4 and 5 cm s^{-1} .

Another indirect test to check the reliability of the above set of parameters comes from the comparison of simulated daytime NO_y speciation using these new parameters (Fig. 7a) and the NO_y speciation calculated from the measured species (Fig. 7b). NO_x is the major component of NO_y , followed by Σ PNs and HNO_3 ; in general the model underestimates the contribution of the NO_x and the Σ ANs derived from isoprene, overestimates the contribution of Σ PNs and HNO_3 , whereas the role of the Σ ANs derived from other species is well reproduced by the model. In any case, the modelled NO_y speciation reported in Fig. 7a is systematically in better agreement with the measured NO_y speciation compared with the results of the model using the “base” parameters that are: $\text{NO}_x = 38.51 \%$; $\text{HNO}_3 = 23.25 \%$, Σ PNs = 22.86 %, Σ ANs from isoprene = 10.26 % and Σ PNs from other species = 5.12 %.

20 4 Conclusions

A new instrument capable of measuring tropospheric Σ PNs and Σ ANs concentrations with laser-induced fluorescence at low pressure has been developed and deployed for the first time during the OP3 field campaign. Although experimental conditions were difficult in the tropical forest environment, the instrument performance was stable and reliable during the entire campaign and Σ PNs and Σ ANs have been successfully measured for the first time in such environment. Several tests, performed to check the selectivity of the system, confirmed that the TD-LIF performs well. During the

4812

OP3 field campaign, maximum and median Σ PNs and Σ ANs concentrations were lower than observed in other forest campaigns. Model simulations showed good agreement between measured and modelled Σ PNs, but overestimations of the observed Σ ANs. A series of sensitivity tests show that the isoprene nitrates chemistry of the MCM model may be the reason for the model overestimation of Σ ANs. The best agreement between measured and modelled Σ ANs can be achieved reducing the isoprene recycling from 100 % to 70 % and the isoprene nitrates yield, coming from the reaction of peroxy nitrates with NO, from 10 % to 5 %. The optimal isoprene nitrates dry deposition is 4 cm s^{-1} . These results suggest an important role of the isoprene nitrates chemistry in the ozone production and aerosol budget in a tropical rain forest similar to what observed in airborne campaigns in other completely different forests in North America.

Acknowledgements. We would like to thank G. Visconti for supporting the instrument development. National Instruments for supporting the L'Aquila group mission in Borneo. Yoshizumi Kajii (Tokyo Metropolitan University) who kindly lent a spare laser for the campaign. We thank Manuela Rastelli for English corrections. We thank the Malaysian and Sabah governments for the permission to conduct research in Malaysia; the Malaysian Meteorological Department for the access to the Bukit Atur GAW station; Waidi Sinun of Yayasan Sabah, Glen Reynolds of the Royal Society's South East Asian Rain Forest Research Programme and Brian Davison of Lancaster University for logistical support. The OP3 project was funded by the UK Natural Environment Research Council (NE/D002117/1). Additional support from the ACCENT Network of Excellence is acknowledged. P. Di Carlo work is supported by Fondazione CARISPAQ. This paper is number 527 of the Royal Society's South East Asian Rainforest Research Programme.

References

- Archibald, A. T., Cooke, M. C., Utembe, S. R., Shallcross, D. E., Derwent, R. G., and Jenkin, M. E.: Impacts of mechanistic changes on HO_x formation and recycling in the oxidation of isoprene, *Atmos. Chem. Phys.*, 10, 8097–8118, doi:10.5194/acp-10-8097-2010, 2010.
- Atkinson, R., Carter, W. P. L., and Winer, A. M.: Effects of temperature and pressure on alkyl

4813

- nitrate yields in the NO_x photooxidations of normal-pentane and normal-heptane, *J. Phys. Chem.*, 87, 2012–2018, 1983.
- Atlas, E., Pollock, W., Greenberg, J., Heidt, L., and Thompson, A. M.: Alkyl nitrates, non-methane hydrocarbons, and halocarbon gases over the equatorial Pacific Ocean during Saga-3, *J. Geophys. Res.*, 98, 16993–16947, 1993.
- Barnes, I., Bastian, V., Becker, K. H., and Tong, Z.: Kinetics and Products of the Reactions of NO₃ with Monoalkenes, Dialkenes, and Monoterpenes, *J. Phys. Chem.*, 94, 2413–2419, 1990.
- Bertman, S. B., Roberts, J. M., Parrish, D. P., Buhr, M. P., Goldan, P. D., Kuster, W. C., and Fehsenfeld, F. C.: Evolution of alkyl nitrates with air mass age, *J. Geophys. Res.*, 100, 22805–22813, 1995.
- Blanchard, P., Shepson, P. B., Schiff, H. I., and Drummond, J. W.: Development of a gas chromatograph for trace level measurement of peroxyacetyl nitrate using chemical amplification, *Anal. Chem.*, 65, 2472–2477, 1993.
- Buhr, M. P., Parrish, D. D., Norton, R. B., Fehsenfeld, F. C., Sievers, R. E., and Roberts, J. M.: Contribution of organic nitrates to the total reactive nitrogen budget at a rural eastern U.S. site, *J. Geophys. Res.*, 95, 9809–9816, 1990.
- Crutzen, P. J.: The role of NO and NO₂ in the chemistry of the troposphere and the stratosphere, *Ann. Rev. Earth Planet Sci.*, 7, 443–472, 1979.
- Damian, V., Sandu, A., Damian, M., Potra, F., and Carmichael, G. R.: The Kinetic PreProcessor KPP – A Software Environment for Solving Chemical Kinetics, *Comput. Chem. Eng.*, 26, 1567–1579, 2002.
- Day, D. A., Wooldridge, P. J., Dillon, M. B., Thornton, J. A., and Cohen, R. C.: A thermal dissociation laser-induced fluorescence instrument for in situ detection of NO₂, peroxy nitrates, alkyl nitrates, and HNO₃, *J. Geophys. Res.*, 107, 4046, doi:10.1029/2001JD000779, 2002.
- Day, D. A., Dillon, M. B., Wooldridge, P. J., Thornton, J. A., Rosen, R. S., Wood, E. C., and Cohen, R. C.: On alkyl nitrates, O₃, and the 'missing NO_y', *J. Geophys. Res.*, 108, 4501, doi:10.1029/2003JD003685, 2003.
- Day, D. A., Wooldridge, P. J., and Cohen, R. C.: Observations of the effects of temperature on atmospheric HNO₃, Σ ANs, Σ PNs, and NO_x: evidence for a temperature-dependent HO_x source, *Atmos. Chem. Phys.*, 8, 1867–1879, doi:10.5194/acp-8-1867-2008, 2008.
- Dari-Salisburgo, C., Di Carlo, P., Giammaria, F., Kajii, Y., and D'Altorio, A.: Laser induced fluorescence instrument for NO₂ measurements: Observations at a central Italy background

4814

- site, *Atmos. Environ.*, 43, 970–977, 2008.
- Emmerson, K. M. and Evans, M. J.: Comparison of tropospheric gas-phase chemistry schemes for use within global models, *Atmos. Chem. Phys.*, 9, 1831–1845, doi:10.5194/acp-9-1831-2009, 2009.
- 5 European Environment Agency (EEA): Air pollution by ozone in Europe in summer 2004, Technical Report 3/2005, Copenhagen, Denmark, available at: <http://reports.eea.eu.int>, 2005.
- Fahey, D. W., Hubler, G., Parrish, D. D., Williams, E. J., Norton, R. B., Ridley, B. A., Singh, H. B., Liu, S. C., and Fehesenfeld, F. C.: Reactive nitrogen species in the troposphere: Measurements of NO, NO₂, HNO₃, particulate nitrate, peroxyacetyl nitrate (PAN), O₃, and total reactive oddnitrogen (NO_x) at Niwot Ridge, Colorado, *J. Geophys. Res.*, 91, 9781–9793, 1986.
- 10 Fahey, D. W.: Application of the NO/O₃ chemiluminescence technique to measurements of reactive nitrogen species in the stratosphere, in *Measurement of Atmospheric Gases: 21–23 January 1991, Los Angeles, California*, edited by: Schiff, H. I., 212–223, Int. Soc. for Opt. Eng., Bellingham, Wash, 1991.
- 15 Farmer, D. K., Wooldridge, P. J., and Cohen, R. C.: Application of thermal-dissociation laser induced fluorescence (TD-LIF) to measurement of HNO₃, Salkyl nitrates, Peroxy nitrates, and NO₂ fluxes using eddy covariance, *Atmos. Chem. Phys.*, 6, 3471–3486, doi:10.5194/acp-6-3471-2006, 2006.
- 20 Farmer, D. K. and Cohen, R. C.: Observations of HNO₃, ΣAN, ΣPN and NO₂ fluxes: evidence for rapid HO_x chemistry within a pine forest canopy, *Atmos. Chem. Phys.*, 8, 3899–3917, doi:10.5194/acp-8-3899-2008, 2008.
- Fehesenfeld, F. C., Dickerson, R. R., Hübler, G., Luke, W. T. L., Nunnermacker, J., Williams, E. J., Roberts, J. M., Calvert, J. G., Curran, C. M., Delany, A. C., Eubank, C. S., Fahey, D. W., Fried, A., Gandrud, B. W., Langford, A. O., Murphy, P. C., Norton, R. B., Pickering, K. E., and Ridley, B. A.: A ground-based intercomparison of NO, NO_x, and NO_y measurement techniques, *J. Geophys. Res.*, 92, 14710–14722, 1987.
- 25 Fiore, A. M., Horowitz, L. A. W., Purves, D. W., Levy, H., Evans, M. J., Wang, Y. X., Li, Q. B., and Yantosca, R. M.: Evaluating the contribution of changes in isoprene emissions to surface ozone trends over the eastern United States, *J. Geophys. Res.-Atmos.*, 110, D12303, doi:10.1029/2004JD005485, 2005.
- 30 Flocke, F., Weinheimer, A. J., Swanson, A. L., Roberts, J. M., Schmitt, R., and Shertz, S.: On the measurement of PANs by Gas Chromatography and Electron Capture Detection, *J.*

4815

- Atmos. Chem.*, 52, 19–43, 2005.
- Fowler, D. E., Nemitz, E., Misztal, P., Di Marco, C., Skiba, U., Ryder, J., Helfter, C., J. Cape, N., Owen, S., Dorsey, J., Gallagher, M. W., Coyle, M., Phillips, G., Davison, B., Langford, B., MacKenzie, R., Muller, J., Siong, J., Dari-Salisburgo, C., Di Carlo, P., Aruffo, E., Giammaria, F., Pyle, J. A., and Hewitt, C. N.: Effects of land use on surface-atmosphere exchanges of trace gases and energy in Borneo: comparing fluxes over oil palm plantations and a rainforest *Phil. Trans. R. Soc. B* 2011 366, 3196–3209, doi:10.1098/rstb.2011.0055, 2011.
- 5 Giacomelli, P., Ford K., Espada, C., and Shepson, P. B.: Comparison of the measured and simulated isoprene nitrate distributions above a forest canopy, *J. Geophys. Res.*, 110, D01304, doi:10.1029/2004JD005123, 2005.
- 10 Guenther, A., Karl, T., Harley, P., Wiedinmyer, C., Palmer, P. I., and Geron, C.: Estimates of global terrestrial isoprene emissions using MEGAN (Model of Emissions of Gases and Aerosols from Nature), *Atmos. Chem. Phys.*, 6, 3181–3210, doi:10.5194/acp-6-3181-2006, 2006.
- 15 Hewitt, C. N., MacKenzie, A. R., Di Carlo, P., Dorsey, J. R., Evans, M., Fowler, D., Gallagher, M. W., Helfter, C., Hopkins, J., Jones, H., Langford, B., Lee, J. D., Lewis, A. C., Lim, S. F., di Marco, C., Misztal, P., Moller, S., Monks, P. S., Nemitz, E., Oram, D. E., Owen, S. M., Phillips, G., Pugh, T., Pyle, J. A., Reeves, C. E., Ryder, J., Siong, J., Skiba, U., Stewart, D. J., and Thomas, R.: Nitrogen management is essential to prevent tropical oil palm plantations from causing ozone pollution, *P. Natl. Acad. Sci.*, 106, 18447–18451, 2009.
- 20 Hewitt, C. N., Lee, J. D., MacKenzie, A. R., Barkley, M. P., Carslaw, N., Carver, G. D., Chappell, N. A., Coe, H., Collier, C., Commane, R., Davies, F., Davison, B., DiCarlo, P., Di Marco, C. F., Dorsey, J. R., Edwards, P. M., Evans, M. J., Fowler, D., Furneaux, K. L., Gallagher, M., Guenther, A., Heard, D. E., Helfter, C., Hopkins, J., Ingham, T., Irwin, M., Jones, C., Karunaharan, A., Langford, B., Lewis, A. C., Lim, S. F., MacDonald, S. M., Mahajan, A. S., Malpass, S., McFiggans, G., Mills, G., Misztal, P., Moller, S., Monks, P. S., Nemitz, E., Nicolas-Perea, V., Oetjen, H., Oram, D. E., Palmer, P. I., Phillips, G. J., Pike, R., Plane, J. M. C., Pugh, T., Pyle, J. A., Reeves, C. E., Robinson, N. H., Stewart, D., Stone, D., Whalley, L. K., and Yin, X.: Overview: oxidant and particle photochemical processes above a south-east Asian tropical rainforest (the OP3 project): introduction, rationale, location characteristics and tools, *Atmos. Chem. Phys.*, 10, 169–199, doi:10.5194/acp-10-169-2010, 2010.
- 30 Hopkins, J. R., Lewis, A. C., and Read, K. A.: A two-column method for long-term monitoring of non-methane hydrocarbons (NMHCs) and oxygenated volatile organic compounds (o-

4816

- VOCs), *J. Environ. Mon.*, **5**, 8–13, 2003.
- Horowitz, L. W., Fiore, A. M., Milly, G. P., Cohen, R. C., Perring, A., Wooldridge, P. J., Hess, P. G., Emmons, L. K., and Lamarque, J. F.: Observational constraints on the chemistry of isoprene nitrates over eastern United States, *J. Geophys. Res.-Atmos.*, **112**, D12S08, doi:10.1029/2006JD007747, 2007.
- 5 Hudman, R. C., Jacob, D. J., Cooper, O. R., Evans, M. J., Heald, C. L., Park, R. J., Fehsenfeld, F., Flocke, F., Holloway, J., Hubler, G., Kita, K., Koike, M., Kondo, Y., Neuman, A., Nowak, J., Oltmans, S., Parrish, D., Roberts, J. M., and Ryerson, T.: Ozone production in transpacific Asian pollution plumes and implications for ozone air quality in California, *J. Geophys. Res.*, **109**, 1–14, 2004.
- 10 Ito, A., Sillman, S., and Penner, J. E.: Effects of additional nonmethane volatile organic compounds, organic nitrates, and direct emissions of oxygenated organic species on global tropospheric chemistry, *J. Geophys. Res.-Atmos.*, **112**, D06309, doi:10.1029/2005JD006556, 2007.
- 15 Jacob, D. J.: Introduction to atmospheric chemistry, Princeton University Press, Princeton, New Jersey, 1999.
- Jenkin, M. E., Saunders, S. M., Wagner, V., and Pilling, M. J.: Protocol for the development of the Master Chemical Mechanism, MCM v3 (Part B): tropospheric degradation of aromatic volatile organic compounds, *Atmos. Chem. Phys.*, **3**, 181–193, doi:10.5194/acp-3-181-2003, 2003.
- 20 Jones, C. E., Hopkins, J. R., and Lewis, A. C.: In situ measurements of isoprene and monoterpenes within a south-east Asian tropical rainforest, *Atmos. Chem. Phys.*, **11**, 6971–6984, doi:10.5194/acp-11-6971-2011, 2011.
- Kroll, J. H., Ng, N. L., Murphy, S. M., Flagan, R. C., and Seinfeld, J. H.: Secondary organic aerosol formation from isoprene photooxidation, *Environ. Sci. Technol.*, **40**, 1869–1877, 2006.
- 25 LaFranchi, B. W., Wolfe, G. M., Thornton, J. A., Harrold, S. A., Browne, E. C., Min, K. E., Wooldridge, P. J., Gilman, J. B., Kuster, W. C., Goldan, P. D., de Gouw, J. A., McKay, M., Goldstein, A. H., Ren, X., Mao, J., and Cohen, R. C.: Closing the peroxy acetyl nitrate budget: observations of acyl peroxy nitrates (PAN, PPN, and MPAN) during BEARPEX 2007, *Atmos. Chem. Phys.*, **9**, 7623–7641, doi:10.5194/acp-9-7623-2009, 2009.
- 30 Langford, B., Misztal, P. K., Nemitz, E., Davison, B., Helfter, C., Pugh, T. A. M., MacKenzie, A. R., Lim, S. F., and Hewitt, C. N.: Fluxes and concentrations of volatile organic com-

4817

- pounds from a South-East Asian tropical rainforest, *Atmos. Chem. Phys.*, **10**, 8391–8412, doi:10.5194/acp-10-8391-2010, 2010.
- Madronich, S.: Photodissociation in the atmosphere, 1, actinic flux and the effects of ground reflections and clouds, *J. Geophys. Res.*, **92**, 9740–9752, 1987.
- 5 MacKenzie, A. R., Langford, B., Pugh, T. A. M., Robinson, N., Misztal, P. K., Heard, D. E., Lee, J. D., Lewis, A. C., Jones, C. E., Hopkins, J. R., Philips, G., Monks, P. S., Karunaharan, A., Hornsby, K. E., Nicolas-Perea, V., Coe, H., Whalley, L. K., Edwards, P. M., Evans, M. J., Stone, D., Ingham, T., Commane, R., Furneaux, L., McQuaid, J., Nemitz, E., Yap Kok Seng, Fowler, D., Pyle, J. A., and Hewitt, C. N.: The atmospheric chemistry of trace gases and particulate matter emitted by different land uses in Borneo, *Philos. T. Roy. Soc. B*, **366**, 3177–3195, doi:10.1098/rstb.2011.0053, 2011.
- 10 Mills, G. P., Sturges, W. T., Salmon, R. A., Bauguitte, S. J.-B., Read, K. A., and Bandy, B. J.: Seasonal variation of peroxyacetyl nitrate (PAN) in coastal Antarctica measured with a new instrument for the detection of sub-part per trillion mixing ratios of PAN, *Atmos. Chem. Phys.*, **7**, 4589–4599, doi:10.5194/acp-7-4589-2007, 2007.
- 15 Munger, J. W., Wofsy, S. C., Bakwin, P. S., Fan, S. M., Goulden, M. L., Daube, B. C., Goldstein, A. H., Moore, K. E., and Fitzjarrald, D. R.: Atmospheric deposition of reactive nitrogen oxides and ozone in a temperate deciduous forest and a subarctic woodland 1. Measurements and mechanisms, *J. Geophys. Res.*, **101**, 12639–12657, 1996.
- 20 Paulot, F., Crouse, J. D., Kjaergaard, H. G., Kroll, J. H., Seinfeld, J. H., and Wennberg, P. O.: Isoprene photooxidation: new insights into the production of acids and organic nitrates, *Atmos. Chem. Phys.*, **9**, 1479–1501, doi:10.5194/acp-9-1479-2009, 2009.
- Parrish, D. D., Buhr, M. P., Trainer, M., Norton, R. B., Shimshock, J. P., Fehsenfeld, F. C., Anlauf, K. G., Bottenheim, J. W., Tang, Y. Z., Wiebe, H. A., Roberts, J. M., Tanner, R. L., Newman, L., Bowersox, V. C., Olszyna, K. J., Bailey, E. M., Rodgers, M. O., Wang, T., Berresheim, H., Rovchoudhury, U. K., and Demerjian, K. L.: Total reactive oxidized nitrogen levels and the partitioning between the individual species at six rural sites in eastern North America, *J. Geophys. Res.*, **98**, 2927–2939, 1993.
- 25 Pearson, G., Davies, F., and Collier, C.: Remote sensing of the tropical rain forest boundary layer using pulsed Doppler lidar, *Atmos. Chem. Phys.*, **10**, 5891–5901, doi:10.5194/acp-10-5891-2010, 2010.
- 30 Perring, A. E., Bertram, T. H., Wooldridge, P. J., Fried, A., Heikes, B. G., Dibb, J., Crouse, J. D., Wennberg, P. O., Blake, N. J., Blake, D. R., Brune, W. H., Singh, H. B., and Cohen, R. C.:

4818

- Airborne observations of total RONO_2 : new constraints on the yield and lifetime of isoprene nitrates, *Atmos. Chem. Phys.*, 9, 1451–1463, doi:10.5194/acp-9-1451-2009, 2009a.
- Perring, A. E., Wisthaler, A., Graus, M., Wooldridge, P. J., Lockwood, A. L., Mielke, L. H., Shepson, P. B., Hansel, A., and Cohen, R. C.: A product study of the isoprene+ NO_3 reaction, *Atmos. Chem. Phys.*, 9, 4945–4956, doi:10.5194/acp-9-4945-2009, 2009b.
- 5 Pugh, T. A. M., MacKenzie, A. R., Hewitt, C. N., Langford, B., Edwards, P. M., Furneaux, K. L., Heard, D. E., Hopkins, J. R., Jones, C. E., Karunaharan, A., Lee, J., Mills, G., Misztal, P., Moller, S., Monks, P. S., and Whalley, L. K.: Simulating atmospheric composition over a South-East Asian tropical rainforest: performance of a chemistry box model, *Atmos. Chem. Phys.*, 10, 279–298, doi:10.5194/acp-10-279-2010, 2010.
- 10 Pugh, T. A. M., Ryder, J., MacKenzie, A. R., Moller, S. J., Lee, J. D., Helfter, C., Nemitz, D., Lowe, D., and Hewitt, C. N.: Modelling chemistry in the nocturnal boundary layer above tropical rainforest and a generalized effective nocturnal ozone deposition velocity for sub-ppbv NO_x conditions, *J. Atmos. Chem.*, 65, 89–110, doi:10.1007/s10874-011-9183-4, 2011.
- 15 Reeves, C. E., Slemr, J., Oram, D. E., Worton, D., Penkett, S. A., Stewart, D. J., Purvis, R., Watson, N., Hopkins, J., Lewism, A., Methven, J., Blake, D. R., and Atlas, E.: Alkyl nitrates in outflow from North America over the North Atlantic during Intercontinental Transport of Ozone and Precursors 2004, *J. Geophys. Res.*, 112, D10S37, doi:10.1029/2006JD007567, 2007.
- 20 Ridley, B. A., Shetter, J. D., Walega, J. G., Madronich, S., Elsworth, C. M., Grahek, F. E., Fehsenfeld, F. C., Norton, R. B., Parrish, D. D., Hobler, G., Buhr, M., Williams, E. J., Allwine, E. J., and Westberg, H. H.: The behaviour of some organic nitrates at Boulder and Niwot Ridge, Colorado, *J. Geophys. Res.*, 93, 13949–13961, 1990.
- Roberts, J. M., Williams, J., Baumann, K., Buhr, M. P., Goldan, P. D., Holloway, J., Hubler, G., Kuster, W. C., McKeen, S. A., Ryerson, T. B., Trainer, M., Williams, E. J., Fehsenfeld, F. C., Bertman, S. B., Nouaime, G., Seaver, C., Grodzinsky, G., Rodgers, M., and Young, V. L.: Measurements of PAN, PPN and MPAN made during the 1994 and 1995 Nashville Intensive on the Southern Oxidant Study: Implications for regional ozone production from biogenic hydrocarbons, *J. Geophys. Res.*, 103, 22473–22490, 1998a.
- 25 Rosen, R. S., Wood, E., Wooldridge, P. J., Thornton, J. A., Day, D. A., Kuster, B., Williams, E. J., Jobson, B. T., and Cohen, R. C.: Observations of total alkyl nitrates during Texas Air Quality Study 2000: Implications for O_3 and alkyl nitrate photochemistry, *J. Geophys. Res.*, 107, D07303, doi:07310.01029/02003JD004227, 2004.

4819

- Rollins, A. W., Kiendler-Scharr, A., Fry, J. L., Brauers, T., Brown, S. S., Dorn, H.-P., Dubé, W. P., Fuchs, H., Mensah, A., Mentel, T. F., Rohrer, F., Tillmann, R., Wegener, R., Wooldridge, P. J., and Cohen, R. C.: Isoprene oxidation by nitrate radical: alkyl nitrate and secondary organic aerosol yields, *Atmos. Chem. Phys.*, 9, 6685–6703, doi:10.5194/acp-9-6685-2009, 2009.
- 5 Saunders, S. M., Jenkin, M. E., Derwent, R. G., and Pilling, M. J.: Protocol for the development of the Master Chemical Mechanism, MCM v3 (Part A): tropospheric degradation of non-aromatic volatile organic compounds, *Atmos. Chem. Phys.*, 3, 161–180, doi:10.5194/acp-3-161-2003, 2003.
- 10 Stone, D., Evans, M. J., Commane, R., Ingham, T., Floquet, C. F. A., McQuaid, J. B., Brookes, D. M., Monks, P. S., Purvis, R., Hamilton, J. F., Hopkins, J., Lee, J., Lewis, A. C., Stewart, D., Murphy, J. G., Mills, G., Oram, D., Reeves, C. E., and Heard, D. E.: HO_x observations over West Africa during AMMA: impact of isoprene and NO_x , *Atmos. Chem. Phys.*, 10, 9415–9429, doi:10.5194/acp-10-9415-2010, 2010.
- 15 Stone, D., Evans, M. J., Edwards, P. M., Commane, R., Ingham, T., Rickard, A. R., Brookes, D. M., Hopkins, J., Leigh, R. J., Lewis, A. C., Monks, P. S., Oram, D., Reeves, C. E., Stewart, D., and Heard, D. E.: Isoprene oxidation mechanisms: measurements and modelling of OH and HO_2 over a South-East Asian tropical rainforest during the OP3 field campaign, *Atmos. Chem. Phys.*, 11, 6749–6771, doi:10.5194/acp-11-6749-2011, 2011.
- 20 Trainer, M., Buhr, M. P., Curran, C. M., Fehsenfeld, F. C., Hsie, E. Y., Liu, S. C., Norton, R. B., Parrish, D. D., Williams, E. J., Gandrud, B. W., Ridley, B. A., Shetter, J. D., Allwine, E. J., and Westberg, H. H.: Observations and modeling of the reactive nitrogen photochemistry at a rural site, *J. Geophys. Res.*, 96, 3045–3063, 1991.
- Turnipseed, A. A., Huey, L. G., Nemitz, E., Stickel, R., Higgs, J., Tanner, D. J., Sluscher, D. L., Sparks, J. P., Flocke, F., and Guenther, A.: Eddy covariance fluxes of peroxyacetyl nitrates (PANs) and NO_y to a coniferous forest, *J. Geophys. Res.*, 111, D09304, doi:10.1029/2005JD006631, 2006.
- von Kuhlmann, R., Lawrence, M. G., Pöschl, U., and Crutzen, P. J.: Sensitivities in global scale modeling of isoprene, *Atmos. Chem. Phys.*, 4, 1–17, doi:10.5194/acp-4-1-2004, 2004.
- Williams, E. J., Roberts, J. M., Baumann, K., Bertman, S. B., Buhr, S., Norton, R. B., and Fehesenfeld, F. C.: Variations in NO_y composition at Idaho Hill, Colorado, *J. Geophys. Res.*, 102, 6297–6314, 1997.
- 30 Williams, E. J., Baumann, K., Roberts, J. M., Bertman, S. B., Norton, R. B., Fehsenfeld, F. C., Springston, S. R., Nunnermacker, L. J., Newman, L., Olszyna, K., Meagher, J., Hartsell,

4820

- B., Edgerton, E., Pearson, J. R., Rodgers, M. O.: Intercomparison of ground-based NO_y measurement techniques, *J. Geophys. Res.*, 103, 22261–22280, 1998.
- Wolfe, G. M., Thornton, J. A., McNeill, V. F., Jaffe, D. A., Reidmiller, D., Chand, D., Smith, J., Swartzendruber, P., Flocke, F., and Zheng, W.: Influence of trans-Pacific pollution transport on acyl peroxy nitrate abundances and speciation at Mount Bachelor Observatory during INTEX-B, *Atmos. Chem. Phys.*, 7, 5309–5325, doi:10.5194/acp-7-5309-2007, 2007.
- Wooldrige, P. J., Perring, A. E., Bertram, T. H., Flocke, F. M., Roberts, J. M., Singh, H. B., Huey, L. G., Thornton, J. A., Wolfe, G. M., Murphy, J. G., Fry, J. L., Rollins, A. W., LaFranchi, B. W., and Cohen, R. C.: Total Peroxy Nitrates (SPNs) in the atmosphere: the Thermal Dissociation-Laser Induced Fluorescence (TD-LIF) technique and comparisons to speciated PAN measurements, *Atmos. Meas. Tech.*, 3, 593–607, doi:10.5194/amt-3-593-2010, 2010.

4821

Table 1. Summary of data inputs of the model.

Compounds	Median (ppt)	Mean (ppt)	Standard deviation (ppt)	Range (ppt)
Ozone	5.7×10^3	5.9×10^3	0.8×10^3	4.9×10^3 to 8.0×10^3
Carbon monoxide	87.5×10^3	88.8×10^3	5.3×10^3	81.3×10^3 to 97.2×10^3
Water	$25\,538.0 \times 10^6$	$25\,535.2 \times 10^6$	457.4×10^6	$24\,215 \times 10^3$ to $26\,272 \times 10^6$
Nitrogen dioxide	204.0	208.1	26.7	173.7 to 261.2
Ethane	240.2	241.0	5.1	234.3 to 252.0
Propane	459.7	476.5	149.7	184.3 to 673.9
Isobutane	352.4	430.8	181.3	270.7 to 906.1
n-Butane	176.6.3	202.3	62.3	133.2 to 373.0
2-Methylbutane	13.9	14.9	4.6	9.3 to 25.0
n-Pentane	15.9	16.0	2.0	13.3 to 19.8
Ethene	58.9	56.7	6.6	47.3 to 65.5
Propene	34.2	73.1	97.3	22.0 to 375.6
But-1-ene	121.3	119.4	7.2	106.6 to 131.3
Methanol	2161.4	2134.5	261.3	1738.1 to 2698.8
Acetaldehyde	65.9	63.4	6.2	49.3 to 68.6
Propan-2-one	389.4	380.0	29.0	298.1 to 412.2
2-Methylbuta-1,3-diene	1371.3	1398.5	630.8	493.6 to 2450.8
α -Pinene	21.5	20.5	2.6	15.5 to 23.1
Acetylene	90.1	89.0	9.6	76.6 to 108.8

4822

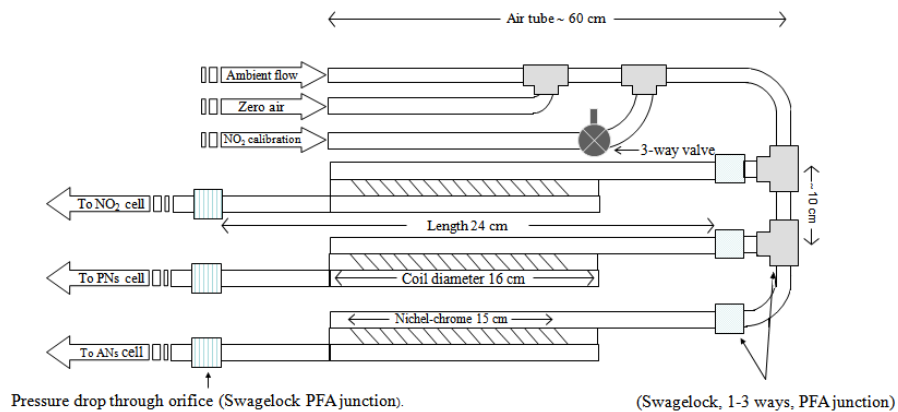


Fig. 1. Schematic of all the components of the inlet system. In the OP3 configuration were used three channels (two heated).

4823

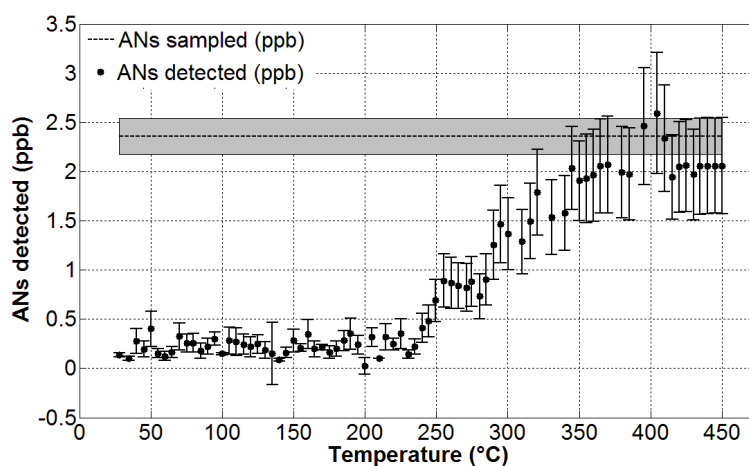


Fig. 2. Laboratory TD-LIF test: known amounts of synthetic N-Propilnitrate sampled by the inlet system as function of the temperature.

4824

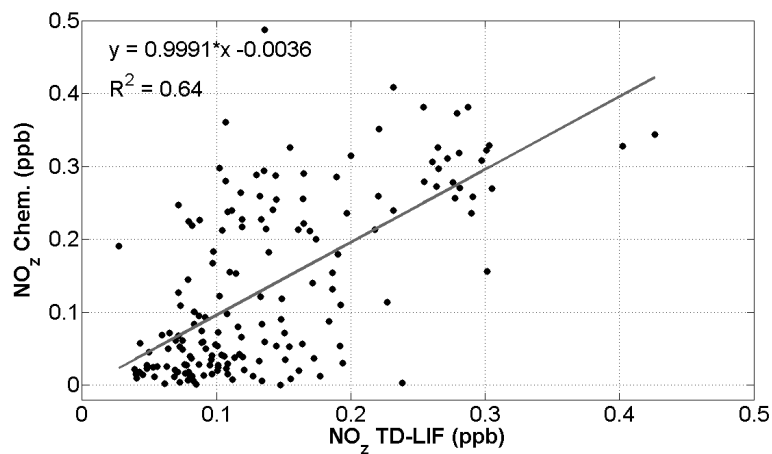


Fig. 3. Intercomparison between NO_2 measured by the Chemiluniscence and NO_2 ($\Sigma\text{PNs} + \Sigma\text{ANs}$) measured by TD-LIF.

4825

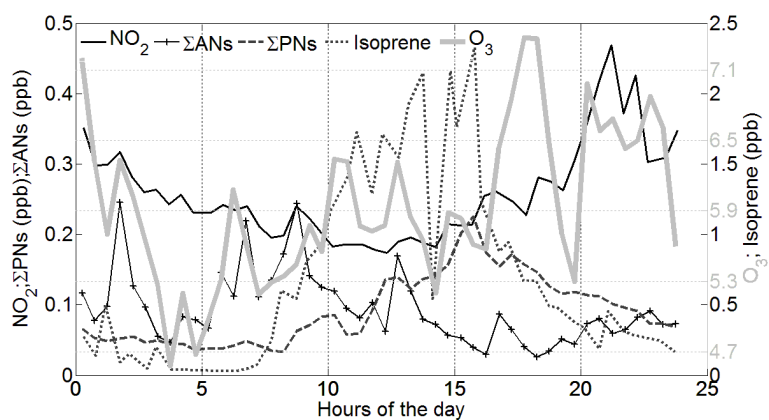


Fig. 4. Diurnal mean of NO_2 , ΣPns , ΣAns , O_3 and isoprene observed at the Bukit Atur tower (8 m above the surface) during OP3 campaign.

4826

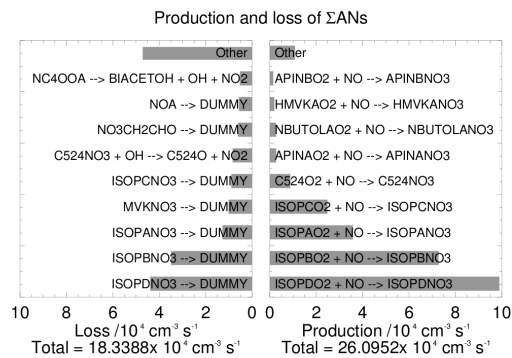
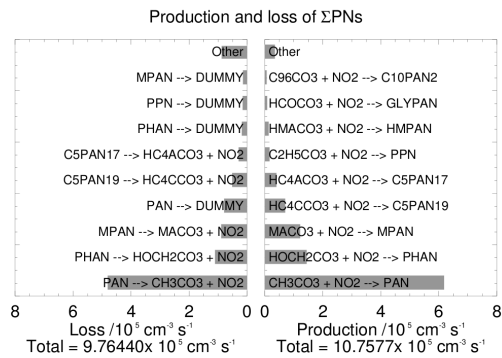


Fig. 5. Upper panel: processes controlling the diurnal production and loss of Σ PNs. Lower panel: as for the upper panel but for Σ ANs. The names of the compounds are specified in the MCM (<http://mcm.leeds.ac.uk>).

4827

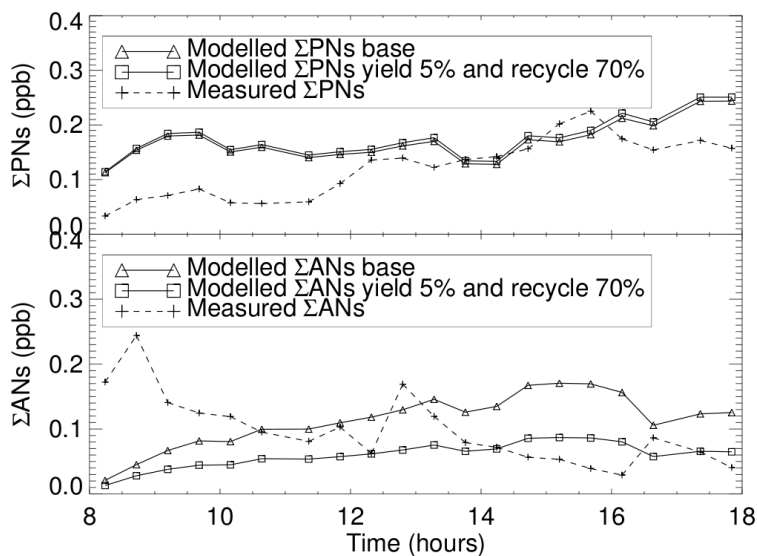


Fig. 6. (A) Time series of measured (plus) and modelled Σ PNs using the MCM default parameters labelled as “base” (triangles) and using a reduced yield (5%) and INs recycling of 70% (squares). **(B)** as for **(A)** but for Σ ANs.

4828

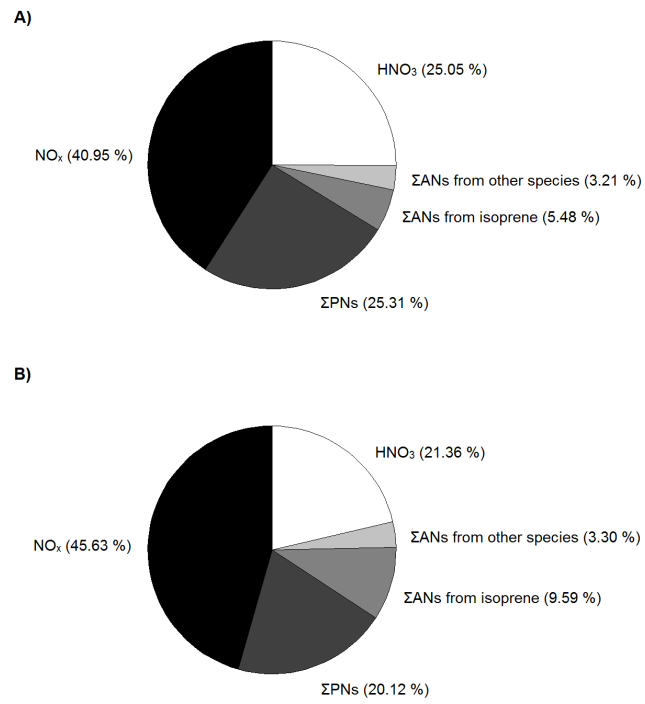


Fig. 7. (A) Daytime simulated NO_y speciation. **(B)** As for **(A)** but using observed NO_y species.